Sādhanā (2020)45:187
https://doi.org/10.1007/s12046-020-01430-1

Experimental investigations of sol-gel process parameters for wear reduction on thermal barrier coated AA2024 aluminum alloys with the use of Taguchi-based optimization

DIPAK KUMAR[1,*] and K N PANDEY[2]

[1]Mechanical Engineering Department, Raj Kumar Goel Institute of Technology (RKGIT), Ghaziabad 201 003, India
[2]Mechanical Engineering Department, Motilal Nehru National Institute of Technology (MNNIT) Allahabad, Prayagaraj 211 004, India
e-mail: dipakmnnit@gmail.com

MS received 24 January 2020; revised 25 May 2020; accepted 30 May 2020

Abstract. The present sol-gel processes present a surface modification technique for improving the sliding wear resistance characteristics of metallic materials of 2024-T351 aluminum alloy. With the help of dip-coating methods, seven weight% yttria stabilized zirconia (7YSZ) as a top-coat is applied over the air plasma sprayed bond-coated materials, CoNiCrAlY, on aluminum alloys. Thereafter, coating thickness is measured using an optical microscope. Further, sliding wear tests are performed on Pin-On-Disc Friction and Wear test rig as per L_{16} orthogonal arrays of Taguchi method. Investigations revealed temperature as the most influencing parameter for uncoated samples while temperature and applied load, both for coated samples. In comparison to base metallic alloys, sol-gel derived YSZ coating on the AA2024 surface exhibited better wear resistance, resulted into the reduction of wear rate.

Keywords. Dry-sliding wear; sol-gel thermal barrier coating; AA2024-T351; Taguchi method.

1. Introduction

Sliding wear is defined as stepwise degradation of material when two bodies are in a contact during relative motion under load [1]. Mechanical system failures under these conditions are subject matter of interest since long time [2]. Various types of metallic alloys are being used in the case of sliding contact of components depending upon the applications [3, 4]. Although it is noticeable that strength of aluminum alloys reduces considerably at high temperature [5–11]. Therefore, wear behavior of Al-Si aluminum alloys, which are used in internal combustion engine components[12, 13], as well as other series of aluminum alloys, e.g., AA 2014 [14], AA 7004-T6 [15], AA 2024-T4 [15], AA 7039 [16] and Al-Si-Cu alloys [17] are studied. In comparison to 2024-T4 AA, low coefficient of friction but with high wear rate in 7 series aluminum alloys against steel disc is reported [15]. But, some researchers are also found lack of adequacy in surface hardness and wear resistance in aluminum alloys and so, are restricted in application to a certain extent [18–20]. Under heat treatable conditions whether it is naturally aged (2024-T4), artificially aged (2024-T6) or both (2024-T351) [21, 22], highest hardness is noted in 2024 AA among all other aluminum alloys, means more beneficial and less critical to wear [22, 23] due to the presence of intermetallic ternary Al-Cu-Mg phase in the form of $CuAl_2$ and $CuMgAl_2$ [21, 24, 25].

For improving wear resistance, there are number of surface protection methods like nitriding, laser gas alloying, electron beam surface alloying, sputtering and duplex surface engineering techniques are found to popular [26–31]. In this direction, there are tremendous work done with application of ceramic materials and found to offer many advantages over metallic materials [3, 4]. Thermal spray techniques for the deposition of ceramic materials forming ceramic oxide coatings such as alumina, zirconia, titania, chromia and silica on the surface are conventionally accepted as surface protection of materials to improve wear and erosion resistance [27, 32]. Among ceramic oxide coating materials, zirconia based ceramics were extensively considered to be a good coating candidate material due to its superior thermo-physical properties [27, 33]. With the tremendous performance of Air Plasma Spraying (APS) in aerospace [34, 35] and internal combustion engines components [34, 36], it was found to be attained more popularity as conventional thermal spray technique to fabricate thermal barrier coating (TBC) on different substrates.

*For correspondence
Published online: 23 July 2020

Therefore, most of the tribological studies of TBC are related to studies on coatings prepared by APS [37–39]. The wear characteristics of zirconia based ceramic coatings were found complicated due to the anisotropic nature of the coatings and, the complexity increased further with the variation of wear factors [40].

From few decades, various researchers have done excellent work on nanostructure coatings and they compared it to plasma spraying technique in all aspects of areas including tribological performance. It was obtained with good toughness, high wear resistance, high hardness, good creep resistance and thermal properties [41–44]. There were lot of difficulties faced during the deposition of nano particle via plasma spraying due to lack of momentum of powder particles. So, spray drying was used for the development of nanoceramic coatings from the nano-powders [45–47]. On other hand, it was also obtained expensive process [48]. Alternatively, sol-gel derived nanostructure coating is observed very economical with low crystallization temperature [49–53]. Thereafter, well established sol-gel technology (SG) with good chemical bonding were successfully obtained [53, 54]. Sol–gel derived alumina coatings produced were found dense, hard, wear and corrosion-resistant ceramic coatings after heat treatment at temperatures as low as 300-500°C [55, 56]. Further, sol-gel derived 60 μm thick alumina coating was successfully applied over grit blasted 25 mm square 6061 aluminum alloy samples [57] and then it were tested to dry sliding wear against both hard bearing steel ball (SAE52100) and mild steel pin (AISI1018 steel) at different sliding speeds and contact loads on Pin-On-Disc apparatus.

To present date, sliding wear of sol-gel based top-coat prepared on bond coated substrates is not reported in the literature and is studied in the present work for the case of AA2024-T351 substrate. Bond coat of intermetallic CoNiCrAlY was fabricated on the substrate by air plasma spraying (APS) [58]. For comparison sliding wear tests were also conducted on uncoated AA2024-T351 substrate. 7 weight % yttria stabilized zirconia sol-gel was synthesized and dip coated as top coat on the bond coated AA2024-T351 aluminum alloy substrate. The tests were performed by selecting four different temperatures (25°C, 150°C, 275°C and 400°C), disc speeds (200 RPM, 400 RPM, 600 RPM and 800 RPM), loads (15N, 30N, 45N and 60N) and sliding velocities (0.5 m/s, 0.6 m/s, 0.7 m/s and 0.8 m/s). Taguchi based orthogonal array (OA) was used for experimentation and an optimal sliding wear parameter were determined for minimum sliding wear rate (SWR) [59].

2. Experimentation

2.1 *Substrate and coating materials*

In the present study, cylindrical pin of 10 mm diameter and 30 mm length of 2024-T351 aluminum alloy was selected as specimen. The chemical composition AA2024-T351 are shown in table 1. Bond coat of CoNiCrAlY on the flat surface of cylindrical substrate were prepared by air plasma spraying at Ms. Anode Plasma Pvt. Ltd., Kanpur (India). The parameters used for APS are shown in table 2. For top-coat, sol-gel of 7YSZ was synthesized and deposited on the bond coated substrate by automatic dip coatings machine (M/s Apex Instrument, Kolkata, Model: dip SV1).

Yttria stabilized zirconia sol was synthesized from zirconium propoxide-acetyl acetone-sulphuric-acid-water-1-propanol system. Precursors used for the yttria stabilized powder synthesis were zirconium(IV)propoxide ($Zr(OPr)_4$) (Aldrich), yttrium(III)nitrates hexahydrate ($Y(NO_3)_3.6H_2O$) (Alfa Aesar), solvent was 1-propanol (SRL). Chelating agents were used as acetyl acetone (AcAc) and Sulphuric acid. Zirconium n-propoxide n-propanol complex ($(C_3H_7O)_4Zr\text{-}C_3H_7OH$) was used as a starting material which was diluted with 1-propanol till the molarity of [Zr] reduced to 0.4M. In the 7YSZ composite sol, 2 weight% Polyvinyl alcohol (2PVA) was mixed and mechanically stirred for making slurry viscous [60]. Dip-coating on the bond coated flat surface of substrate was performed at controlled dipping and withdrawal speed of 250 mm/min [61]. After dipping for 25 minutes, samples were withdrawn and heated at 60°C for 15 minutes. This process was repeated for 150 cycles. After fabrication of top coat, it was dried at room temperature [60].

2.2 *Preparation of samples for wear rate of uncoated AA2024 substrate*

The wear test samples for uncoated substrate were grounded using SiC emery paper from No. 220 to 2000. After grinding of uncoated samples, it was lapped to get the surface finish in the range of Ra 0.023-0.029 μm. After lapping samples were washed by acetone. Finally, cleaned samples were dried and weighed using an electronic balance (Make: CONTECH, 224D) having a resolution of 0.01 mg [60].

2.3 *Preparation of samples for wear test of coated samples*

Heat treated AA2024-T351 SGTBC substrates were dried at 120°C, followed by 220°C, 340°C, 400°C for 8 h to increase the strength of the coating and reduce the roughness. Finally, sol-gel deposited top-coat aluminum alloy substrates were aged for 24 h at 60°C before wear testing. The coatings obtained were found to be smooth with

Table 1. Chemical Composition of AA2024-T351substrate.

Elements	Cu	Mg	Si	Zn	Mn	Al
Compositions (%)	4.7	1.4	0.5	0.25	0.5	Balance

Table 2. Spraying Process Parameters for bond coat of CoNiCrAlY.

Current (A)	Voltage (V)	Primary gas, Ar (l/min)	Secondary gas, H_2 (l/min)	Powder feed rate (g/min)	Spray distance (mm)	Travel speed (mm/sec)
550	67	43	9.5	20	100	30

roughness of coating between 3-4 μm Ra. Finally, samples were dried and weighed using an electronic balance (Make: CONTECH, 224D) of resolution 0.01 mg.

2.4 *Taguchi design of experiments*

Selection of optimal process parameters is very significant for obtaining improved quality characteristics. To achieve one, it required large number of experiments. Taguchi [61] has proposed different orthogonal arrays (OA) to reduce number of experiments and is exceptionally realistic for complex processes. The experimental data were examined on the basis of signal–to-noise ratio (SNR) [62, 63]. This quality characteristic is a smaller-the-better type of performance characteristics as smaller wear rate will be better [59]. Four control factors namely temperature, disc speed, load and sliding velocity were selected for performing experiments are given in table 3. In this experimental study, L_{16} orthogonal array (OA) is selected as there are four control factors with four levels and is summarized in table 4. Pin-On-Disc tests were conducted as per the levels of control factors given in table 4 for both uncoated and coated AA2024-T351 substrate. After conducting tests, SNR for both coated and uncoated samples were calculated on the basis of the equation (1) which is used for the cases of smaller-the-better type of quality characteristic/objective function [59, 62, 63].

$$S/R = -10\log\left[(1/n)\Sigma\left(y_i^2\right)\right] \quad (1)$$

where n is the number of observations (test runs); y_i is the observed data. Further, a statistical analysis of variance (ANOVA) was performed to check the statistically significance sliding wear conditions. Analysis of influence of each sliding wear parameter was carried out by using statistical tool box MINITAB 16.0.

Table 3. Control factors for Sliding Wear experiment and their levels.

Codes	Control factors	Levels			
		L_1	L_2	L_3	L_4
A	Temperature (°C)	25	150	275	400
B	Disc speed (RPM)	200	400	600	800
C	Normal load (N)	15	30	45	60
D	Sliding speed (m/sec)	0.5	0.6	0.7	0.8

2.5 *Sliding wear test*

Dry sliding wear tests were performed on coated specimens (Ø10 mm ×30 mm long pin) against EN31 steel disc using pin-on-disc type wear testing machine (Ducom Pvt. Ltd, Bangalore, India) as per the ASTM standard G99-04. For uncoated samples, after every 10 minute of test run, weight of the samples was measured and the wear debris were removed to avoid presence of debris between the contacting surfaces. In the case of sol-gel TBC samples, samples were cleaned off from loose debris using compressed air and re-weighed till the loss of coating. The wear testing was done thrice to ensure the repeatability of the test and an average of three was selected. The wear rates (g/N.m) were calculated as the ratio of wear mass loss in gram divided by the applied load and sliding distance [64]. Weight loss of both coated and uncoated samples during the wear test was measured using an electronic balance with a resolution of ± 0.01 mg. Wear tested uncoated AA2024-T351 samples and coated AA2024-T351 samples are shown in figures 1 and 2, respectively.

3. Results and discussion

3.1 *Analysis of effect of control factors on sliding wear*

The sixteen experimental test runs conducted as per table 4 are summarized in figure 3 for uncoated AA2024-T351 aluminum alloys and 7YSZ sol-gel coated AA2024-T351 aluminum alloy substrates. Under all test run conditions, the sliding wear rate of uncoated aluminum alloy is more than coated samples. For the case of uncoated samples, sliding wear is maximum under test run conditions of 1 (test run 1) when temperature was 25°C, disc speed was 200 RPM, sliding speed was 0.5 m/sec and applied load was 15N (figure 3). With the increase in temperature wear rate decreases for fixed load conditions. At fixed load of 15 N, for uncoated sample, wear rate is minimum for test run 16, when temperature was 400°C, disc speed was 800 rpm, sliding speed was 0.7 m/sec. For coated and uncoated samples, wear rate is maximum under test run 1 when parameters are temperature 25°C, normal load of 15 N, disc speed of 200 rpm and sliding velocity of 0.5 m/sec. At high temperature of 400°C and for uncoated samples wear rate is minimum for test run 16 when disc speed was 800 rpm, normal load was 15 N and sliding velocity was 0.7 m/sec.

Table 4. Experimental design matrix using L_{16} orthogonal array.

	Levels				Sliding Wear Rate ($\times 10^{-6}$ g/Nm)		Smaller-the-better S/N ratios (SNR)	
Test run	A	B	C	D	2024	SGTBC	2024	SGTBC
1	25	200	15	0.5	0.925	0.876	0.677	1.149
2	25	400	30	0.6	0.551	0.117	5.176	18.636
3	25	600	45	0.7	0.385	0.134	8.291	17.457
4	25	800	60	0.8	0.251	0.163	12.006	15.756
5	150	200	30	0.7	0.184	0.169	14.704	15.442
6	150	400	15	0.8	0.292	0.181	10.692	14.846
7	150	600	60	0.5	0.196	0.124	14.155	18.132
8	150	800	45	0.6	0.176	0.0463	15.089	26.688
9	275	200	45	0.8	0.123	0.0319	18.202	29.924
10	275	400	60	0.7	0.129	0.107	17.788	19.412
11	275	600	15	0.6	0.168	0.118	15.494	18.562
12	275	800	30	0.5	0.124	0.053	18.132	25.514
13	400	200	60	0.6	0.180	0.080	14.895	21.938
14	400	400	45	0.5	0.174	0.071	15.189	22.975
15	400	600	30	0.8	0.156	0.0368	16.137	28.683
16	400	800	15	0.7	0.141	0.079	17.016	22.047
						Average of SNR	13.353	19.823

Figure 1. Worn surface of uncoated AA2024-T351 substrate.

Figure 2. Worn surface of coated AA2024-T351 substrate.

At high temperature of 400°C, for coated samples, sliding wear rate was maximum for test run 13 and minimum for test run 15. At test run 15 other test parameters were disc speed of 600 rpm, normal load of 30 N and sliding velocity of 0.8 m/sec. At maximum testing temperature of 400°C, maximum wear rate for coated and uncoated samples was observed at maximum applied load of 60 N. Wear rate was found to be decreased linearly with increase in disc speed and decreased in applied load. One thing was common at 400°C for a coated sample was that wear rate was almost constant for all sliding velocities except at 0.8 m/sec. In general, wear rate of coated sample decreased with increase in temperature. There are effects of interactions of different parameters of test runs given in table 4 and to get the effect of interactions, if any and optimal control factors Taguchi design of experimental is applied.

3.2 *Optimization of control factors for wear rate*

Results of the sliding wear experiments conducted as per L_{16} orthogonal array of Taguchi is given in table 4 for both uncoated AA 2024 aluminum alloy substrate and 7YSZ sol-gel coated TBC. Signal to Noise Ratio (SNR) were calculated as per the expression for "the-smaller-the-better" type of optimization expressed by equation (1). SNR for uncoated and coated samples are also given in table 4. The average of the SNR for each control factor at each level is given in table 5a for uncoated AA2024-T351 and in table 5b for 7YSZ sol-gel coating on AA 2024-T351. In tables 5a and 5b, Δ is the difference between largest and

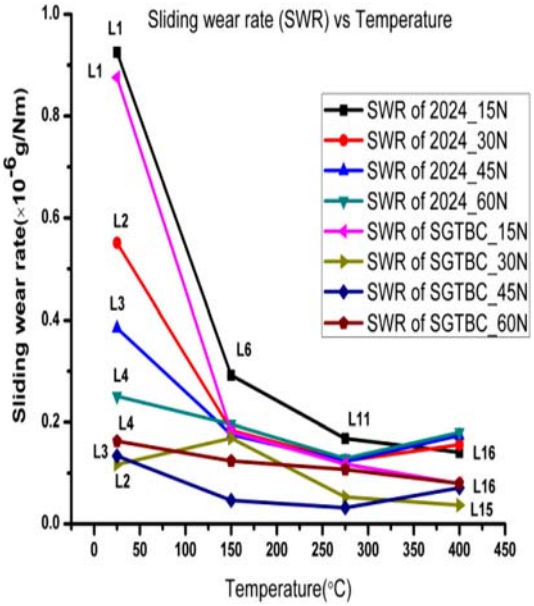

Figure 3. Effect of temperature on wear rate of uncoated and coated substrate.

smallest average SNR for a particular control factor. From this difference, percentage contribution which is a ratio of Δ and summation of Δ of all control factors is calculated. For the case of uncoated samples, (table 5a) the percentage contribution ratio is maximized for temperature. Further, it was concluded that from the results, the most influencing factor for minimization of wear rate is temperature, followed by load, disc speed and sliding speed. With the application of 7YSZ sol-gel coating, the temperature was again observed as most influencing factor for minimization of wear rate that followed by load, disc speed and sliding speed. The average of SNR for each level of control factors in shown in figures 4a and b, for uncoated and coated AA 2024-T351 samples, respectively.

Figures 4a and b also show that temperature is the most dominant performance characteristics among all other factors for both aluminum alloys and sol-gel coated aluminum alloys. Better performance is obtained at A_3 level of temperature and thus the lowest wear rate for uncoated aluminum alloys. The temperature sensitivity of 2024-T351 aluminum alloys increased the hardness, hence resulted in reduction of wear rate at 275°C but with further increase in temperature up to 400°C the wear rate increases. Whereas for coated sample (figure 4b), wear rate decreases up to 400°C showing complete protection of metallic substrate by the application of YSZ sol-gel coating that indicates that nanostructured sol-gel coating improves the wear resistance in comparison to uncoated metallic substrate AA2024-T351. Due to sliding action in wear testing, frictional heat generated is partially delivered into the 7YSZ coating layer as 7YSZ coating materials is low thermal conductivity. This may be due to formation of hard ceramic oxide in the

Table 5a. SNR for Sliding Wear Rate (SWR) of AA2024 substrate.

	Control factors			
Level	Temperature	Disc speed	Load	Sliding speed
1	A_1 = 6.537	B_1 = 12.119	C_1= 10.969	D_1= 12.038
2	A_2 = 13.660	B_2 = 12.211	C_2 = 13.537	D_2 = 12.664
3	A_3 = **17.404**	B_3 = 13.519	C_3 = 14.193	D_3 = **14.449**
4	A_4 = 15.809	B_4 = **15.561**	C_4 = **14.711**	D_4 = 14.259
Δ_{Factor} = Difference of Max. & Min.	10.867	3.442	3.742	2.411; Δ_{Total} = 20.462
Contribution Ratios (%) = $\Delta_{Factor}/\Delta_{Total}$	53.11	16.82	18.29	11.78
Rank	1	3	2	4

Table 5b. SNR for Sliding Wear Rate of AA2024 SGTBC.

	Control factors			
Level	Temperature	Disc speed	Load	Sliding speed
1	A_1 = 13.249	B_1 =17.113	C_1 =14.151	D_1 = 16.943
2	A_2 = 18.777	B_2 =18.967	C_2 = 22.068	D_2 = 21.456
3	A_3 =23.353	B_3 =20.708	C_3 = **24.261**	D_3 = 18.589
4	A_4 =**24.161**	B_4 = **22.501**	C_4 = 18.809	D_4= **22.302**
Δ_{Factor} = Difference of Max. & Min.	10.912	5.388	10.110	5.359; Δ_{Total} = 31.769
Contribution Ratios (%) = $\Delta_{Factor}/\Delta_{Total}$	34.35	16.96	31.82	16.87
Rank	1	3	2	4

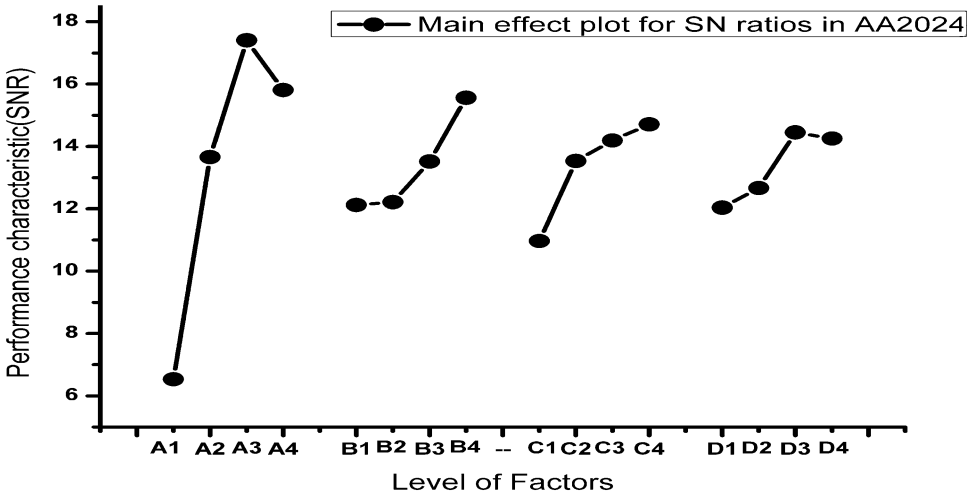

Figure 4a. The effect of design parameters of A, B, C and D on sliding wear behavior of uncoated AA2024-T351.

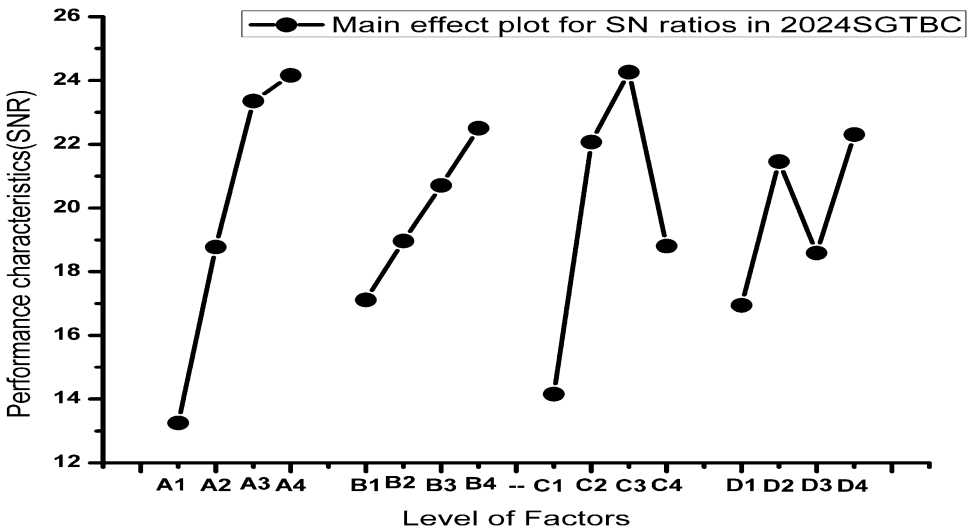

Figure 4b. Effect of design parameters of A, B, C and D on sliding wear behavior of sol-gel (SG) coated 7YSZ ceramics AA2024-T351 aluminum alloy substrate.

contact region [65, 66] which might be attributed to better wear resistance for coated substrate than uncoated one at high temperature. Yan *et al* [67] also pointed out low wear rate at high temperature (200°C) compared to that of room temperature and 100°C testing conditions when Mg-alloys was treated for pin specimen against stainless steel disc.

For parameter B (disc speed), fourth level B_4 is having highest average SNR for both uncoated and coated samples, figures 4a and b. For uncoated and coated samples, lowest average SNR is for 200 RPM disc speed (B_1) indicating highest wear rate of aluminum alloys and highest value of average SNR is for 800 RPM disc speed showing lowest wear resistance at this value. The reduction in the wear rate with the increase of disc speed may be attributed to the development of frictional heating during wear testing. AA 2024-T351 has inherent properties of formation of $CuMgAl_2$ intermetallic alloys [68] layers at high temperature which resists the developed heat with the increase of sliding speed. One important behavior is noticed in sliding wear rate is insensitive to variation of speed for both coated and uncoated samples.

For control parameter C (applied load) high performance characteristics is for fourth level of parameter C (i.e., applied load of 60 N) therefore wear rate will be minimum

Table 6. Optimum Control factors of Sliding wear Rate in uncoated AA2024 and 7YSZ SGTBC.

Control factors				
	Temperature	Disc speed	Load	Sliding speed
AA2024 substrate				
Optimum level	A_3	B_4	C_4	D_3
Optimum value	275°C	800RPM	60N	0.7 m/sec
2024SGTBC				
Optimum level	A_4	B_4	C_3	D_4
Optimum value	400°C	800RPM	45N	0.8 m/sec

at this level of parameter C for the case of uncoated aluminum alloy substrate and third level of applied load i.e., 45 N was observed for low wear rate in SG7YSZ TBC. It is observed that, regardless of the magnitude of the applied load, the uncoated substrate has a much higher wear rate than that of the coated substrate [3]. It is cleared that forces developed might be principally controlled by the manner of material removal in YSZ ceramic materials [27].

For both coated and uncoated samples, the wear rate, in general, decreases with the increase in applied load. In the case of coated samples, wear rate suddenly increases at 60N applied load (C_4). Singh *et al* [69] also reported rapid increase in wear at higher load in the range of 50-80 N for APS deposited alumina coating against EN32 steel disc. This adverse effect at high load range is due to establishment of differential thermal stress into the coating due to low thermal conductivity of 7YSZ coatings. When the load on the pin is increased at 60N, the actual area of contact would increase towards nominal area, resulting in increase of frictional force between two mating surfaces. The increased frictional force and surface area of coated sample in contact bring higher wear rate. In the case of uncoated pin sample and steel disc, wear rate is decreased with increase of load, indicating that hardness of uncoated pin sample increased with increasing of load due to high temperature effects during testing.

Similarly, third level of parameter D, i.e., 0.7 m/s sliding velocity shows the higher performance characteristics, (figure 4a) indicating low wear rate in the uncoated aluminum alloy substrate. For the case of 7YSZ sol-gel coating, the fourth level of sliding speed i.e., 0.8 m/sec is having the highest performance characteristics and thus lowest wear rate. From the current dry sliding wear tests, it is also realized that the wear rate is low at the high sliding speed as compared to the low sliding speed (figures 4a and b). With the increase in sliding velocity, time available for frictional heat dissipation from contact surfaces to atmosphere is very less. This friction heating in the contact zone must be accelerating the formation of oxidize layer of ceramic giving better performance at high sliding velocity [64]. Although, at third level of sliding velocity, i.e., 0.7 m/s, wear rate is in comparison to second level i.e., 0.6 m/s sliding velocity. This may be due to interaction effect of different parameters.

In order to obtain minimum wear rate in uncoated aluminum alloys, the optimum level of parameters is temperature A_3 (275°C), disc speed B_4 (800 RPM), applied load C_4 (60N) and sliding velocity D_3 (0.7 m/sec). For the case of coated substrate, the optimum level of parameters is temperature A_4 (400°C), disc speed B_4 (800 RPM), load C_3 (45 N) and sliding velocity D_4 (0.8 m/sec). These values are summarized in table 6 also. It was observed that the presence of a sol-gel derived 7YSZ coating significantly reduces the sliding wear rate in compared to uncoated metallic alloy substrate.

In order to obtain the influence of each parameter on wear rate on uncoated and coated aluminum alloys substrate, analysis of variance (ANOVA) were applied. The results of ANOVA for both the cases are presented in tables 7a and b, respectively using the statistical tool box Minitab 16. One can observe from these results that all the design parameters (i.e., control factors) of wear rate have a bearing on the average value.

The percentage contribution ratio of each control factor for uncoated and coated aluminum alloys substrate are shown in figures 5a and b, respectively. Significance parameter for both the cases are also shown in figure 6 based on average SNR for each control factors.

3.3 *Confirmation experiment*

The confirmation experiment is the last step in the design of experiment process. Through confirmation test, optimized control factors are validated. The confirmation tests were performed on two sets of optimal control factors namely $A_3B_4C_4D_3$ and $A_4B_4C_3D_4$ to predict the sliding wear rate of uncoated and SG coated 7YSZ AA2024 (SGTBC) substrate, respectively. The wear rate at optimum control factors (figure 4a) of $A_3B_4C_4D_3$ for uncoated AA2024-T351 substrate was obtained as 0.115 ($\times 10^{-6}$g/Nm) which is less than the lowest wear rate of 0.123 for control factor levels $A_3B_1C_3D_4$ reported in table 4. The SNR at optimized control factors was 22.06, whereas for $A_3B_1C_3D_4$ (table 4) control factors was 18.202. The improvement in SNR was

Table 7a. Analysis of variance (ANOVA) for S/N ratios for Sliding Wear Rate of AA2024 substrate.

Factors	DOF	Sum of square	Variance	F-ratio	Percentage contribution	P-value	Importance
A (Temperature)	3	275.956	91.985	33.50	77.35	0.008	Most Significant
B (Impact angle)	3	30.908	10.303	3.75	8.66	0.153	Not significant
C (Impact velocity)	3	33.053	11.018	4.01	9.26	0.142	Not significant
D (Erodent flow rate)	3	16.913	5.638	2.05	4.73	0.285	Not significant
Error	3	8.238	2.746				
Total	15	365.067		43.31			

Table 7b. Analysis of variance (ANOVA) for S/N ratios for Sliding Wear Rate of AA2024 SGTBC.

Factors	DOF	Sum of square	Variance	F-ratio	Percentage contribution	P-value	Importance
A (Temperature)	3	293.90	97.97	8.18	44.26	0.059	Significant
B (Disc speed)	3	64.13	21.38	1.78	9.64	0.323	Not significant
C (Load)	3	231.75	77.25	6.45	34.90	0.080	Significant
D (Sliding velocity)	3	74.53	24.84	2.07	11.20	0.282	Not significant
Error	3	35.94	11.98				
Total	15	700.25		18.48			

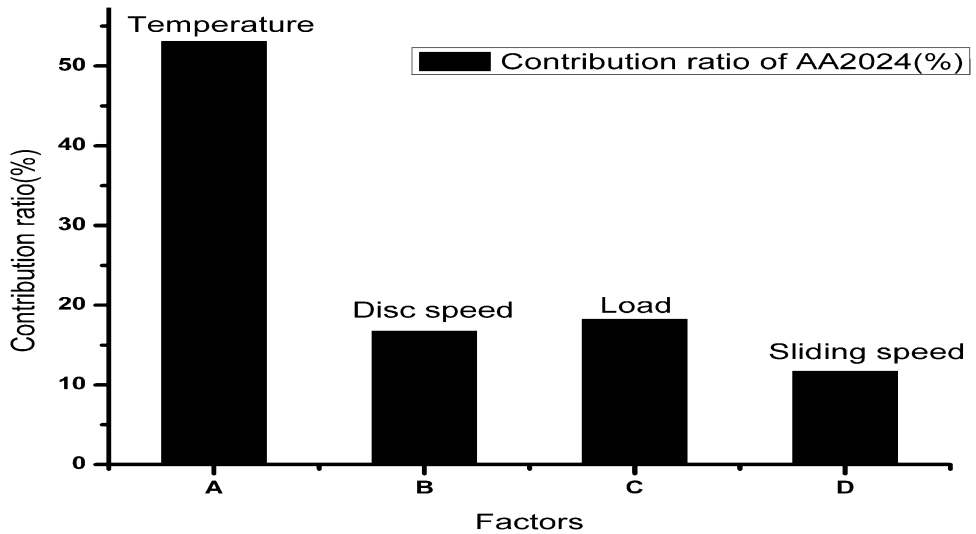

Figure 5a. The contribution ratio of each control factors of uncoated AA2024-T351.

0.584 dB (table 8). Level $A_3B_1C_3D_4$ is corresponding to minimum wear obtained for the case of sol-gel coated samples (Test run no. 9 in table 4). Similarly, confirmation test was conducted at optimum control factors (figure 4b) of $A_4B_4C_3D_4$ for 7YSZ sol-gel coating. Sliding wear rate at this level of experimental parameters was 0.0232 ($\times$ 10^{-6} g/N.m) which is minimum among all test results shown in table 4 for coated samples. As per table 4, minimum wear rate is corresponding of control factors $A_3B_1C_3D_4$ and it is 0.0319 ($\times 10^{-6}$ g/Nm) for coated sample. The SNR was 32.690 dB which was also more than the presented SNR in table 4. Improvement in SNR with respect to sliding wear rate at control parameter $A_3B_1C_3D_4$ is 2.766 dB. The SNR can also be predicted for sliding wear rate in uncoated metallic aluminum alloys AA2024 substrate with the help of equation (2) [59]

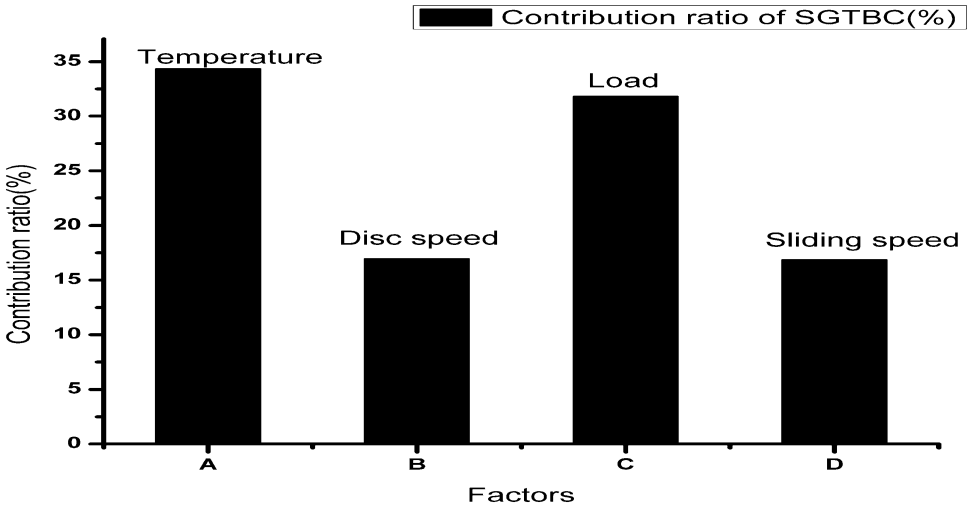

Figure 5b. The contribution ratio of each control factors of coated AA2024SGTBC.

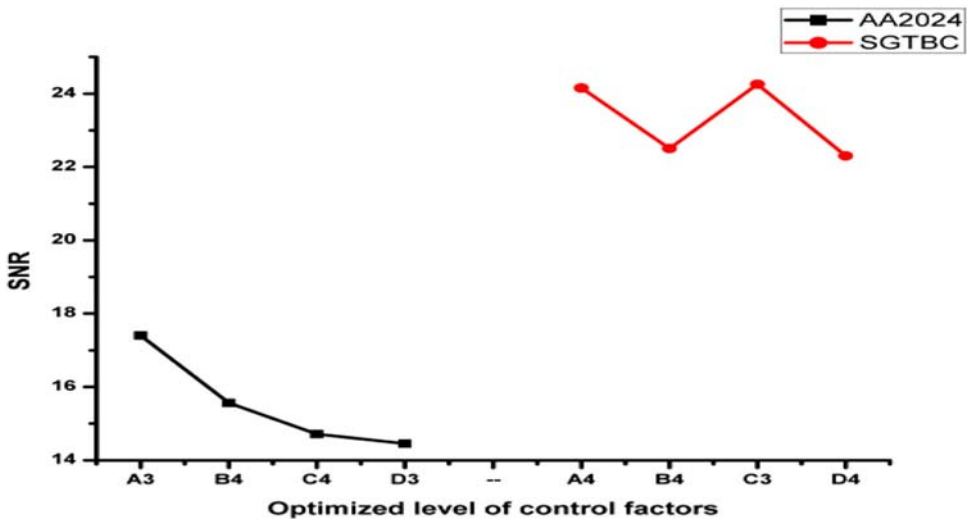

Figure 6. Optimal combination of control factors for uncoated AA2024 and coated 2024SGTBC.

Table 8. Results of the Confirmation Experiments for Sliding Wear Rate in AA2024.

Level	Initial Parameters $A_3B_1C_3D_4$	Optimum Parameters	
		$A_3B_4C_4D_3$ (Prediction)	$A_3B_4C_4D_3$ (Experimental)
Sliding wear rate	0.123 (g/Nm)	–	0.115 ($\times 10^{-6}$ g/Nm)
SNR (dB)	18.202 dB	22.066 dB	18.876 dB
Improvement of S–N ratio for Erosive wear rate = 18.786 – 18.202 = 0.584 dB			

$$(\eta_{2024})_{\mathrm{Pr}\,ediction} = \bar{T} + (\bar{A}_3 - \bar{T}) + (\bar{B}_4 - \bar{T}) + (\bar{C}_4 - \bar{T}) + (\bar{D}_3 - \bar{T}) \quad (2)$$

Where $\bar{T}$ is the average of SNR values equal to 13.353 as given in table 4 and $\bar{A}_3$, $\bar{B}_4$, $\bar{C}_4$, $\bar{D}_3$are average SNR at levels A_3, B_4, C_4 and D_3 as given in table 5a. Similarly, the estimated SNR for sliding wear rate in AA2024 SGTBC

Table 9. Results of the Confirmation Experiments for Sliding Wear rate in AA2024 SGTBC.

Level	Initial Parameters $A_3B_1C_3D_4$	Optimum Parameters	
		$A_4B_4C_3D_4$ (Prediction)	$A_4B_4C_3D_4$ (Experimental)
Sliding Wear Rate	0.0319 ($\times 10^{-6}$ g/Nm)	–	0.0232 ($\times 10^{-6}$g/Nm)
SNR (dB)	29.924 dB	33.756 dB	32.690 dB
Improvement of S–N ratio for Sliding Wear Rate = 32.69 – 29.924 = 2.766 dB			

can be calculated by the following predictive equation (3) [59]

$$(\eta_{SGTBC})_{\mathrm{Pr}\,ediction} = \bar{T} + (\bar{A}_4 - \bar{T}) + (\bar{B}_4 - \bar{T}) + (\bar{C}_3 - \bar{T}) + (\bar{D}_4 - \bar{T}) \quad (3)$$

Where $\bar{T}$ = 19.823 dB is average SNR value as given in table 4 and $\bar{A}_4$, $\bar{B}_4$,$\bar{C}_3$ and $\bar{D}_4$ are average SNR at these levels of control factors as given in table 5b. The predicted SNR are also given in tables 8 and 9 for uncoated and coated samples respectively. The predicted SNR value were found to 22.066 dB and 33.756 dB for uncoated and coated samples, respectively.

4. Conclusions

The current investigation presents the influence of sol-gel formulation for yttria stabilised zirconia via dip coating, that was deposited on bond coated aluminum alloys, in sliding wear testing. The following conclusions were concluded after the sliding wear test of the both uncoated and sol-gel YSZ coating using Taguchi based approach.

- The existence of 7YSZ sol-gel coating markedly reduced the wear rate at the all testing parameters except at high load of 60 N and 0.7 m/sec sliding speed.
- Comparatively low wear rate of coating showed the forces acted in mating area are basically depended on the method of material removal in YSZ ceramic materials.
- Micro brittle fracture was observed as coating failures mode, indicated proof of presence of porosity in sol-gel.
- The most influential parameter for sliding wear rate was temperature with percentage contribution ratio of 77.35% and 44.26% for both uncoated and coated AA2024, respectively. The optimum experimental parameters for uncoated substrate and coated substrate are $A_3B_4C_4D_3$ and $A_4B_4C_3D_4$, respectively.
- Comparatively less severity of wear on coatings was attributed to the mechanical contact circumstances and the coating strength as two independent reasons that monitor the wear characteristics of the coating.

References

[1] Deuis R L, Subramanian C and Yellup J M 1997 Dry sliding wear of aluminum composites -A review. *Compos. Sci. Technol.* 57: 415-435

[2] Meyveci A, Karacan I, Aıgulu U C and Durmus H 2010 Pin-on-disc characterization of 2xxx and 6xxx aluminium alloys aged by precipitation age hardening. *J. Alloy Comp.* 491: 278–283

[3] Miller W S, Zhunag L, Bottema J, Wittebrood A J, Smet P D, Haszler A and Vieregge A 2000 Recent development in aluminium alloys for the automotive industry. *Mater. Sci. Eng. A* 280: 37−49

[4] Brown K R, Venie M S and Woods R A 1995 The increasing use of aluminium in automotive applications. *J. Mineral Metal. Mater. Soc.* 47: 20−23

[5] Sahoo K L and Pathak B N 2009 Solidification behaviour, microstructure and mechanical properties of high Fe-containing Al–Si–V alloys. *J. Mater. Process. Technol.* 209: 798–804

[6] Humphreys E S, Warren P J, Titchmarsh J M and Cerezo A 2001 Microstructure and chemistry of Al–V–Fe-Si nano quasi crystalline alloys. *Mater. Sci. Eng. A* 304-306: 844–848

[7] Wang Z J, Wu L, Qi Y, Cai W and Jiang Z 2010 Self-lubricating Al_2O_3/PTFE composite coating formation on surface of aluminum alloys. *Surf. Coat. Technol.* 204:3315–3318

[8] Rao R N, Das S, Mondal D P, Dixit G and Devi S L T 2013 Dry sliding wear maps for AA7010 (Al-Zn-Mg-Cu) aluminium matrix composite. *Tribol. Int.* 60:77–82

[9] Ozdemir I, Tekmen C, Tsunekawa Y and Grund T 2010 Wear behavior of plasma-sprayed Al-Si/TiB_2/h-BN composite coatings. *J. Therm. Spray Technol.* 19:384–391

[10] Al-Qutub A M, Khalil A, Saheb N and Hakeem A S 2013 Wear and friction behavior of Al 6061 alloy reinforced with carbon nanotubes. *Wear* 297: 752–761

[11] Shi H W, Han E H, Liu F C and Kallip S 2013 Protection of 2024-T3 aluminium alloy by corrosion resistant phytic acid conversion coating. *Appl. Surf. Sci.* 280:325–331

[12] Kanth V K, Parmilla Bai B N and Viswas S K 1990 Wear mechanisms in a hypereutectic Al-Si alloy sliding against steel. *Scripta Metallurg. et Materialia* 24: 267–272

[13] Liu Y, Asthana R and Rohatgi P K 1991 A map for wear mechanism in aluminum alloys. *J. Mater. Sci.* 26: 99–102

[14] Bishop D P, Li X Y, Tandon K N and Caley W F 1998 Dry sliding wear behavior of aluminum alloy 2014 micro-alloyed with Sn and Ag. *Wear* 222: 84–92

[15] Iwai Y, Hou W, Honda T and Yoneda H 1996 Wear behavior of high tensile strength aluminum alloys under dry and lubricated conditions. *Wear* 196: 46–53

[16] Mindivan H, Baydogan M, Sabri Kayali E and Cimenoglu H 2005 Wear behaviour of 7039 aluminum alloy. *Mater. Character.* 54: 263–269

[17] Lozano D E, Mercado-Solis R D, Perez A J, Talamantes J, Morales F and Hernandez-Rodriguez M A L 2009 Tribological behaviour of cast hypereutectic Al–Si–Cu alloy subjected to sliding wear. *Wear* 267:545–549

[18] Günzel R, Wieser E, Richter E and Steffen J 1994 Plasma source ion implantation of oxygen and nitrogen in aluminum. *J. Vac. Sci. Technol.* B 12: 927–930

[19] Xia L, Wang R, Ma X and Sun Y 1994 Structure and wear behavior of nitrogen-implanted aluminum alloys. *J. Vac. Sci. Technol.* B 12: 931–934

[20] Zhan Z, Ma X, Feng L, Sun Y and Xia L 1998 Tribological behavior of aluminum alloys surface layer implanted with nitrogen ions by plasma immersion ion implantation. *Wear* 220: 161–167

[21] Cavali M N and Mandava V 2008 Effect of temperature and ageing time on 2024 aluminum behavior. In: *Proceeding of 6th International congress and exposition*. June 2–5, Orlando, Florida, USA, p. 1–5

[22] Starke E A Jr and Staley J T 1996 Application of modern aluminum alloys to aircraft. *Prog. Aerospace Sci.* 32: 131–172

[23] Meriç C 2000 An investigation on the elastic modulus and density of vacuum cast aluminum alloy 2024 containing lithium additions. *J. Mater. Eng. Perform.* 9: 266–271

[24] Fine M A 1975 Precipitation hardening of aluminum alloys. *Metallurgical Trans. A* 6A: 625–630

[25] Atik E, Meriç C and Karlik B 1996 Determination of yield strength of 2014 aluminium alloy under ageing conditions by means of artificial neural networks method. *Math. Comput. Appl.* 1:16–20

[26] Spies H J 2010 Surface engineering of aluminium and titanium alloys: an overview. *Surf. Eng.* 26: 126–134

[27] Kar S, Kumar S, Bandyopadhyay P P and Paul S 2020 Grindability of plasma sprayed thermal barrier coating using super abrasive wheel. *Transactions of the IMF* 98: 30–36

[28] Gangopadhyay S, Acharya R, Chattopadhyay A K and Paul S 2009 Pulsed DC magnetron sputtered MoSx–TiN composite coating for improved mechanical properties and tribological performance. *Surf. Coat. Technol.* 203: 3297–3305

[29] Kumar D and Pandey K N 2014 Study on thermal fatigue behavior of plasma sprayed yttria zirconia thermal barrier coatings (TBCs) systems on aluminum alloy. *Int. J. Mech. Prod. Eng*. 2: 19–22

[30] Sargade V G, Gangopadhyay S, Paul S and Chattopadhyay A K 2011 Effect of coating thickness on the characteristics and dry machining performance of TiN film deposited on cemented carbide inserts using CFUBMS. *Mater. Manuf. Process.* 26: 1028–1033

[31] Kumar D, Shree G and Dwivedi V 2020 Wear and hardness evaluation of electrodeposited Ni-SiC nanocomposite coated copper. *Int. J. Microstr. Mater. Proper.* 15: 87–106

[32] Wang Y, Jiang S, Wang M, Wang S, Danny X and Strut Peter R 2000 Abrasive wear characteristics of plasma sprayed nanostructured alumina titania coatings. *Wear* 237: 176–185

[33] Kose R, Urtekin L, Findik F and Salman S 2006 An investigation of different ceramic coating thermal properties. *Mat. Des.* 27: 585–590

[34] Jong-Han S, Dae-Soon L and Hyo-Sok A 2000 Effect of annealing and Fe_2O_3 addition on the high temperature tribological behavior of the plasma sprayed yttria-stabilized zirconia coating. *Surf. Coat. Technol.* 133–134: 403–410

[35] Ouyang J H, Sasaki S and Umeda K 2001 Low-pressure plasma-sprayed ZrO_2CaF_2 composite coating for high temperature tribological applications. *Surf. Coat. Technol.* 137: 21–30

[36] Li J F, Liao H, Wang X Y, Normand B, Ji V, Ding C X and Coddet C 2004 Improvement in wear resistance of plasma sprayed yttria stabilized, zirconia coating using nanostructured powder. *Tribol. Int.* 37:77–84

[37] Westergård R, Axén N, Wiklund U and Hogmark S 2000 An evaluation of plasma sprayed ceramic coatings by erosion, abrasion and bend testing. *Wear* 246:12–19

[38] Giovanni B, Valeria C, Luca L and Tiziano M 2006 Wear behaviour of thermally sprayed ceramic oxide coatings. *Wear* 261:1298–1315

[39] Kumar D and Pandey K N 2016 Study on dry sliding wear characteristics of air plasma spraying (APS) deposited CoNiCrAlY intermetallic coatings on aluminium alloy substrate. *Int. J. Surf. Sci. Eng.* 10: 303–316

[40] Ramachandran C S, Balasubramanian V, Ananthapadmanabhan P V and Viswabaskaran V 2012 Understanding the dry sliding wear behaviour of atmospheric plasma-sprayed rare earth oxide coatings. *Mater. Des.* 39: 234–252

[41] Darut G, Ageorges H, Denoirjean A and Fauchais P 2013 Tribological performances of YSZ composite coatings manufactured by suspension plasma spraying. *Surf. Coat. Technol.* 217:172–180

[42] Hongqing L, Youtao X, Kai L, Liping H, Shansong H, Bizeng Z and Xuebin Z 2014 Microstructure and wear behavior of graphene nanosheets-reinforced zirconia coating. *Ceram. Int.* 40:12821–12829

[43] Gammel F J, Jonke D P and Rohr O 2004 *Nano powders–An approach to enhanced surface coatings.* Springer Netherlands: Kluwer Academic Publisher: 261–72

[44] Fauchais P 2004 Understanding plasma spraying. *J. Phys. D: Appl. Phys.* 37:86–108

[45] Sanchez E, Bannier E, Cantavella V, Salvador M D, Klyatskina E, Morgiel J, Grzonka J and Boccaccini A R 2008 Deposition of Al_2O_3–TiO_2 nanostructured powders by atmospheric plasma spraying. *J. Therm. Spray Technol.* 17: 329–337

[46] Fauchais P, Montavon G and Bertrand G 2010 From powders to thermally sprayed coatings. *J. Therm. Spray Technol.* 19: 56–80

[47] Viswanathan V, Rea K E, Vaidya A and Seal S 2008 Role of spray drying of nano agglomerates in morphology evolution in nanostructured APS coatings. *J. Amer. Ceram. Soc.* 91:379–386

[48] Cao X Q, Vaseen R, Schwartz S, Jungen W, Tietz F and Stoever D 2000 Spray-drying of ceramics for plasma-spray coating. *J. Europ. Ceram. Soc.* 20: 2433-2439

[49] Viazzi C, Bonino J P and Ansart F 2006 Synthesis by sol-gel route and characterization of yttria stabilized zirconia coatings for thermal barrier applications. *Surf. Coat. Technol.* 201:3889-3893

[50] Kumar D and Pandey K N 2017Thermo-structural analysis of sol-gel route based yttria stabilized zirconia tetragonal zirconia (YSTZ) powders for thermal barrier applications. *Ind. J. Chem. Technol.* 24: 153-161

[51] Brinker CJ and Sherer GW 1990 *Sol-gel Science: the physics and chemistry of sol-gel processing,* Academic Press, San Diego (Elsevier)

[52] Brinker C J, Ashley C S, Cairncross R A, Chen K S, Hurd A J, Reed S T, Samuel J, Randall PS, Schwartz R W and Scotto C S1996 Sol-gel derived ceramic films- fundamentals and applications. *Metallur. Ceram. Protect. Coat*. Chapman & Hall, London 112–151 (ISBN: 978-94-010-7171-0)

[53] Barrow D A, Petroff T E and Sayer M 1996 *Method for producing thick ceramic films by a sol-gel coating process.* US Patent No. US 5585136 A

[54] Barrow D A, Petroff T E and Sayer M 1995 Thick ceramic coatings using a sol-gel based ceramic-ceramic 0-3 composite. *Surf. Coat. Technol.* 76–77:113–118

[55] Thai T T, Trinh A T, Olivier M G 2020 Hybrid sol-gel coatings doped with cerium nanocontainers for active corrosion protection of AA2024. *Prog. Org. Coatings* 138: 01–11

[56] Troczynski T and Yang Q 1999 *Process for making chemically bonded sol-gel ceramic*. US Patent No.US 6284682 B1

[57] Wilson S, Hawthorne H M, Yang Q and Troczynski T 2000 Sliding and abrasive wear of composite sol-gel alumina coated Al alloys. *Surf. Coat. Technol.* 133–134: 389–396

[58] Kumar D, Pandey K N and Das D K 2018 Characterization of air plasma based 7YSZ aluminum alloys thermal barrier systems for hot zone. *Proc. I. Mech. Eng. Part L: J. Mater. Des. Appl*. 232: 582-591

[59] Kosal S, Ferit F, Kayikcs R and Savas O 2012 Experimental optimization of dry sliding wear behavior of in situ AlB_2/Al composite based on Taguchi's method. *Mater. Des.* 42: 124–130

[60] Kumar D 2019 Comparison of thermal fatigue of superni 718SGTBCs and APS TBCs. *Trans. India. Inst. Metals* 72:1927–1939

[61] Sniezewski J, LeMaoult Y, Lours P, Pin L, Bekale V M, Monceau D, Oquab D, Fenech J, Ansart F and Bonino J P 2010 Sol-gel thermal barrier coatings: Optimization of the manufacturing route and durability under cyclic oxidation. *Surf. Coat. Technol.* 205: 1256–1261

[62] Roy R K 2001 DOE using the Taguchi approach. Wiley, New York

[63] Kumar D and Pandey K N 2017 Optimization of the process parameters in generic thermal barrier coatings using the Taguchi method and grey relational analysis. *Proc. I. Mech. Eng. Part L J. Mat. Des. Appl*. 231: 600–610

[64] Ahn H S and Kwon O K 1993 Wear behavior of plasma-sprayed partially stabilized zirconia on a steel substrate. *Wear* 162–164: 636–644

[65] Kennedy F E Jr 1984 Thermal and thermomechanical effects in dry sliding. *Wear* 100: 453–476

[66] Quinn T F J and Winter W O 1985 The thermal aspects of oxidational. *Wear* 102: 67–80

[67] Yan G Z-R, Min-Xian W, Yu-Tao Z and Shu-Qi W 2011 Dry sliding wear behavior and mechanism of AM60B alloy at 25−200°C. *Trans. Nonferrous Met. Soc. China* 21: 2584–2591

[68] Ming-Kai T and Nam P S 1977 Chemical effects in sliding wear of aluminum. *Wear* 44: 145–162

[69] Singh V P, Sil A and Jayaganthan R 2011 A study on sliding wear and erosive wear behavior of atmoshpheric plasma sprayed conventional and nanostructured alumina coatings. *Mater. Des.* 32: 584–591